ELSEVIER

NeuroImage

www.elsevier.com/locate/ynimg
NeuroImage 32 (2006) 989–994

Topography of the human corpus callosum revisited—Comprehensive fiber tractography using diffusion tensor magnetic resonance imaging

Sabine Hofer[a,b,*] and Jens Frahm[a]

[a]*Biomedizinische NMR Forschungs GmbH am Max-Planck-Institut für biophysikalische Chemie, 37070 Göttingen, Germany*
[b]*Bernstein Center for Computational Neuroscience, 37073 Göttingen, Germany*

Received 21 March 2006; revised 19 May 2006; accepted 23 May 2006
Available online 18 July 2006

Several tracing studies have established a topographical distribution of fiber connections to the cortex in midsagittal cross-sections of the corpus callosum (CC). The most prominent example is Witelson's scheme, which defines five vertical partitions mainly based on primate data. Conventional MRI of the human CC does not reveal morphologically discernable structures, although microscopy techniques identified myelinated axons with a relatively small diameter in the anterior and posterior third of the CC as opposed to thick fibers in the midbody and posterior splenium. Here, we applied diffusion tensor imaging (DTI) in conjunction with a tract-tracing algorithm to gain cortical connectivity information of the CC in individual subjects. With DTI-based tractography, we distinguished five vertical segments of the CC, containing fibers projecting into prefrontal, premotor (and supplementary motor), primary motor, and primary sensory areas as well as into parietal, temporal, and occipital cortical areas. Striking differences to Witelson's classification were recognized in the midbody and anterior third of the CC. In particular, callosal motor fiber bundles were found to cross the CC in a much more posterior location than previously indicated. Differences in water mobility were found to be in qualitative agreement with differences in the microstructure of transcallosal fibers yielding the highest anisotropy in posterior regions of the CC. The lowest anisotropy was observed in compartments assigned to motor and sensory cortical areas. In conclusion, DTI-based fiber tractography of healthy human subjects suggests a modification of the widely accepted Witelson scheme and a new classification of vertical CC partitions.

Keywords: DTI; Human brain; Primary motor cortex; Fractional anisotropy

Introduction

The corpus callosum (CC) is by far the largest fiber bundle in the human brain interconnecting the two cerebral hemispheres with more than 300 million fibers. Surgical transection of the CC in humans provides evidence of its important role in interhemispheric functional integration communicating perceptual, cognitive, learned, and volitional information. Most of the fibers serve homotopic interconnections between the hemispheres, but a number of heterotopic fibers also asymmetrically link functionally different cortical areas (Clarke and Zaidel, 1994; De Lacoste et al., 1985; Witelson, 1989). The CC is one of the few white matter tracts that can be discretely identified by conventional MRI. It has been the target of extensive studies (e.g., see Thompson et al., 2003) indicating that its morphology may be related to dyslexia (von Plessen et al., 2002), Tourette's syndrome (Plessen et al., 2004), Down's syndrome (Teipel et al., 2003), depression (Lacerda et al., 2005), schizophrenia (Narr et al., 2002), and HIV/AIDS (Thompson et al., 2006).

Due to the fact that there are no macroscopic anatomical landmarks that clearly delimit distinct callosal areas in a midsagittal cross-section, several geometric partitioning schemes have been designed to subdivide the CC (Duara et al., 1991; Larsen et al., 1992; Weis et al., 1993; Rajapakse et al., 1996). In fact, most studies rely on Witelson's classification, although the underlying data predominantly originates from non-human primates (Witelson, 1989). This scheme defines five vertical callosal segments based on specific arithmetic fractions of the maximum anterior–posterior extent. In particular, the CC is subdivided into regions comprising the anterior third, the anterior and posterior midbody, the posterior third, and the posterior one-fifth. Compartments of the anterior third, including the rostrum, genu, and rostral body, are assigned to prefrontal, premotor, and supplementary motor cortical areas. Fibers originating in the motor cortex are assumed to cross the CC through the anterior midbody, whereas somaesthetic and posterior parietal fiber bundles cross the CC through the posterior midbody. Compartments of the posterior third, including the isthmus and splenium, are assigned to temporal, parietal, and occipital cortical regions. It should be noted, however, that neither Witelson's classification nor other geometric partitioning schemes exactly mirror the texture of the CC at the cellular level.

Light microscopic examinations of the fiber composition in the human CC (Aboitz et al., 1992) revealed a well-defined micro-

* Corresponding author. Fax: +49 551 201 1307.
E-mail address: shofer1@gwdg.de (S. Hofer).
Available online on ScienceDirect (www.sciencedirect.com).

1053-8119/$ - see front matter © 2006 Elsevier Inc. All rights reserved.
doi:10.1016/j.neuroimage.2006.05.044

structure with a consistent pattern of regional differentiation. The density of fibers with a small diameter is most pronounced in the anterior CC (genu), decreases to a minimum in the posterior midbody, and increases again toward the posterior CC (splenium). In contrast, fibers with a large diameter show a diametrically opposed pattern with a peak density in the posterior midbody. Absolute fiber density decreases from the genu to the posterior midbody, increases when entering the splenium, and is diminished again in the most posterior splenial region.

The development of magnetic resonance diffusion tensor imaging (DTI) in conjunction with fiber tractography has opened new possibilities in the research of white matter anatomy. The approach provides unique access to in vivo information about the topography of major fiber tracts and even their maturation during ontogeny (Huang et al., 2005; Dougherty et al., 2005; Ramnani et al., 2004). The method is based on the fact that the MRI-detectable diffusivity of water molecules depends on the principal orientation of the fiber tracts within white matter. Diffusion-weighted MRI sequences probe such mobility along multiple directions in order to fully characterize its orientational distribution within an image voxel. Under the assumption that this distribution may be mathematically represented by a tensor, the principle axis of the corresponding diffusion ellipsoid coincides with the direction of the greatest diffusion coefficient, which then can be identified with the orientation of the underlying fiber bundle. Anisotropy measures reflect the degree to which diffusion is preferred along this direction relative to other directions. Here, fractional anisotropy (FA) values have been used as scalar indicators of the directionality and coherence of fiber tracts (Basser and Pierpaoli, 1996).

The goal of this study was to complement structural assessments of the CC by cortical connectivity information in individual subjects by means of a geometrically undistorted DTI technique without sensitivity to susceptibility differences (Nolte et al., 2000; Rieseberg et al., 2005) in conjunction with a simple algorithm for tract tracing (Mori et al., 1999). A region-of-interest (ROI) to ROI tractography method was employed to identify all trajectories that cross individual pixels within the entire CC (first ROI) and penetrate selective cortex areas (second ROI). This strategy resulted in a detailed separation of transcallosal fiber tracts with respect to their specific cortical projections. In addition, the approach allowed for an assignment of the distribution of FA values to functionally distinct CC regions.

Methods

Participants

A total of eight right-handed human subjects (4 female, 4 male; age range 21−47 years) participated in the study. None of them had any history of neurological abnormality. Handedness was assessed in accordance to the hand preference score reported by Oldfield (1971). All subjects gave written informed consent before each MRI examination.

Data acquisition

MRI studies were conducted at 2.9 T (Siemens Trio, Erlangen, Germany) using an 8-channel phased-array head coil. Acquisitions were performed at 2 mm isotropic resolution using diffusion-weighted single-shot stimulated echo acquisition mode (STEAM) MRI sequences and 5/8 partial Fourier encoding in combination with a projection onto convex subjects (POCS) reconstruction algorithm (Rieseberg et al., 2005). The protocol comprised 24 independent diffusion gradient directions and b values of 0 and 1000 s/mm^2. A total of 50 transverse sections (2 mm thickness) covered the CC and the upper part of the brain. The acquisition time per data set was approximately 9 min. To increase the signal-to-noise ratio, the acquisition was repeated three times. Anatomic images were based on a T_1-weighted 3D fast low angle shot (FLASH) MRI sequence (repetition time TR = 11 ms, echo time TE = 4.9 ms, flip angle 15°).

Fiber tractography

Before calculation of the diffusion tensor the diffusion-weighted images were smoothed with a 3D Gaussian filter (σ = 2 mm). Estimates of axonal projections were computed by the fiber assignment by continuous tracking (FACT) algorithm (Mori et al., 1999). Tracking terminated when the FA value was lower than 0.15 or the main diffusion directions in consecutive steps differed by more than 40° (empirically optimized thresholds). Axonal projections were traced in both anterograde and retrograde directions. All ROIs were manually defined on color-coded maps of the main diffusion direction. The first ROI was placed in a midsagittal plane to define the entire CC. The second target ROI was placed close to the cortex in a transverse section to separate the transcallosal projections into prefrontal, premotor (and supplementary motor), primary motor, primary sensory, parietal, temporal, and occipital regions. The DTI analysis relied on software developed in-house (M. Küntzel).

Parcellation of the corpus callosum

We arrived at a parcellation of the corpus callosum by introducing vertical subdivisions – similar to the Witelson classification – but with respect to the outcome of the fiber tractography. In the midsagittal section of the CC, a geometric baseline was defined by connecting the most anterior and posterior points of the CC. After fiber tracking, the CC regions crossed by fibers belonging to defined cortical areas provided a natural segmentation. The maximum anterior and posterior extent of a segment were used as border lines and projected onto the baseline. The callosal parietal, temporal, and occipital fiber bundles overlapped and could not be separated by vertical lines. They constitute the most posterior region of the CC.

Fractional anisotropy

Quantitative measures of diffusion anisotropy were evaluated in the midsagittal and the two directly neighboring CC sections. In every subject, we determined the mean FA values averaged across the three sections for each cortical region as defined by fiber tractography. To account for interindividual differences in absolute anisotropy and to facilitate group comparisons, the data were normalized to the mean of all FA values in the CC of the respective subject. We then calculated the mean and standard deviation of the normalized FA values of every CC region across subjects. Regional differences were tested for significance (Superior Performing Software System, SPSS Inc.) using ANOVA combined with a post hoc test (Scheffe's test for multiple comparisons) at a threshold of $P < 0.05$.

Results and discussion

Topography of callosal fiber tracts

DTI-based tractography allowed us to reconstruct comprehensive sets of callosal fiber bundles projecting to the cortical hemispheres in all subjects. By classifying tracts according to their cortical projections, we could distinguish between fibers associated with prefrontal, premotor (combined with supplementary motor), primary motor, primary sensory, parietal, temporal and occipital cortical regions. The resulting topology of fiber bundles in the CC is demonstrated in Figs. 1A–C for a single subject using 3D views of respective tracts as well as in Fig. 2 for all subjects by outlining the regional distribution of fibers from all discernable projection areas that cross the midsagittal CC.

The mapping of the callosal radiation, by which corresponding cortical areas of opposite hemispheres are connected, was achieved in much more detail than described before (Huang et al., 2005) and, for example, accounts for a clear separation of callosal primary motor and sensory fiber bundles. Most importantly, however, fibers originating in the motor cortex were found to cross the CC through its posterior half. This is shown in more detail in Figs. 1D and E again using 3D views of complete fiber tracks (single subject) and in Fig. 2 by selectively marking the callosal motor fibers in the midsagittal plane (all subjects). The region of the CC associated with the frontal cortex appears enlarged up to the two-thirds when compared to Witelson's classification. Fibers originating in cortical areas posterior to the motor cortex pass the CC through the remaining posterior one third.

One of the most striking differences compared with the Witelson scheme is that callosal motor and sensory fiber bundles cross the CC in a much more posterior location. These discrepancies between the DTI-based fiber topology of the human CC and Witelson's classification as the standard segmentation stimulated us to suggest a new scheme. As shown in Fig. 3, the proposed arrangement of subdivisons still represents a rather

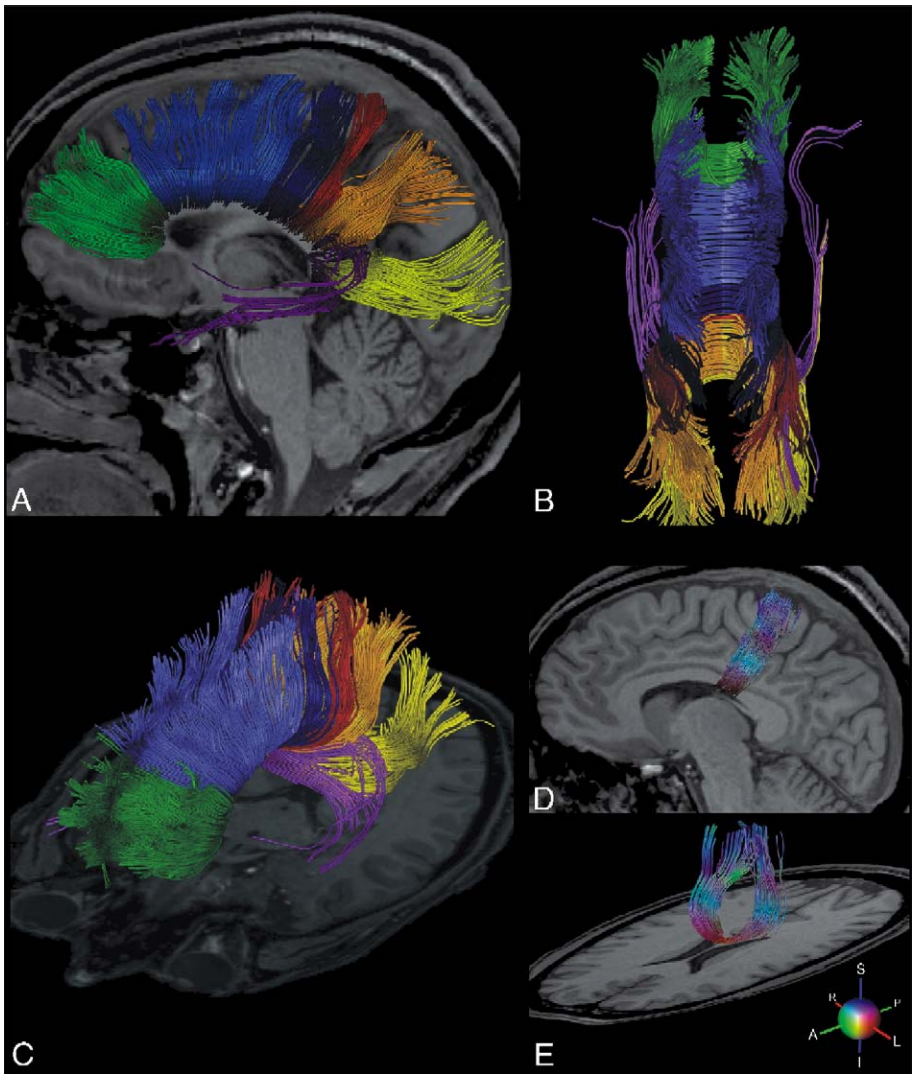

Fig. 1. Transcallosal fiber tracts from a single male subject overlaid onto individual anatomical reference images. (A–C) Sagittal, top, and oblique views of a 3D reconstruction of all callosal fibers comprising bundles projecting into the prefrontal lobe (coded in green), premotor and supplementary motor areas (light blue), primary motor cortex (dark blue), primary sensory cortex (red), parietal lobe (orange), occipital lobe (yellow), and temporal lobe (violet). (D and E) Sagittal and oblique views of callosal fiber tracts that project into the primary motor cortex. The colors correspond to the local mean diffusion direction as indicated by the color code in the lower right of the figure: A, anterior; I, inferior; L, left; P, posterior; R, right; S, superior.

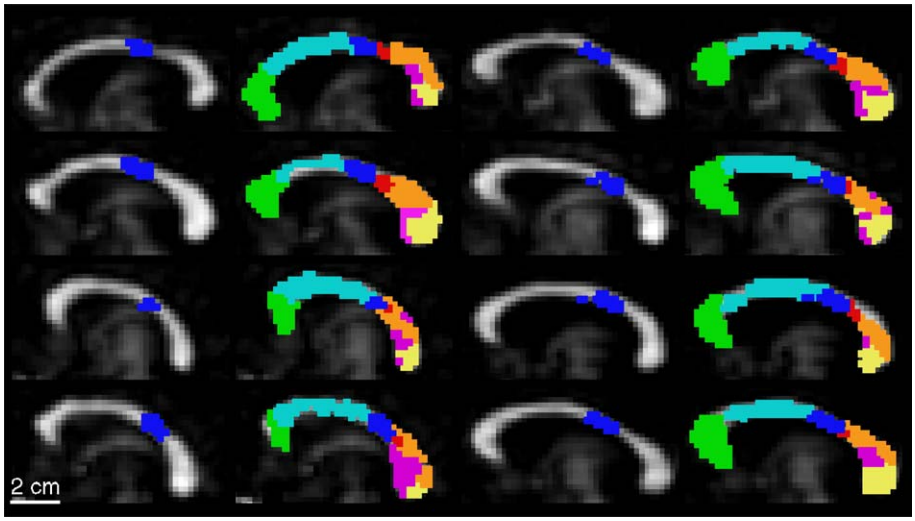

Fig. 2. Fractional anisotropy maps of the midsagittal corpus callosum (grayscale ranging from black for FA = 0 to white for FA = 0.8) with overlay of motor fibers only (left columns) and all discernable fibers projecting into specific cortical areas (right columns). The data were obtained for (left side) 4 female and (right side) 4 male subjects. The color scheme is identical to that of Figs. 1A–C comprising fibers projecting into the prefrontal lobe (green), premotor and supplementary motor areas (light blue), primary motor cortex (dark blue), primary sensory cortex (red), parietal lobe (orange), occipital lobe (yellow), and temporal lobe (violet).

simple view of the CC's internal structure but closely reflects the tract topology. Witelson divided the midsagittal CC geometrically into the anterior third (region I containing fibers projecting into prefrontal, premotor and supplementary motor regions), the anterior midbody (region II with callosal motor fiber bundles), posterior midbody (region III with somaesthetic, posterior parietal projections), isthmus (region IV with posterior parietal, superior temporal projections), and the splenium (region V with occipital, inferior temporal projections).

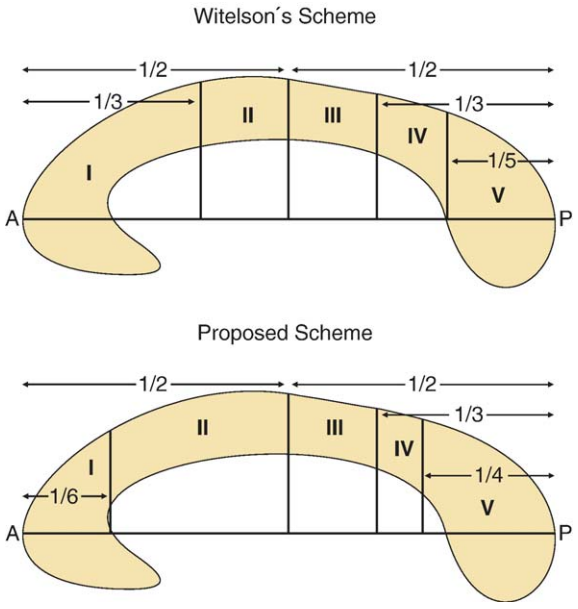

Fig. 3. Topography of the midsagittal corpus callosum. (Top) Witelson's classification. (I) Anterior third: prefrontal, premotor, and supplementary motor; (II) anterior midbody: motor; (III) posterior midbody: somaesthetic, posterior parietal; (IV) isthmus: posterior parietal, superior temporal; (V) splenium: occipital, inferior temporal. A, anterior; P, posterior. (Bottom) Proposed new classification. Region I: prefrontal; region II: premotor and supplementary motor; region III: motor; region IV: sensory; region V: parietal, temporal, and occipital. A, anterior; P, posterior.

Similar to Witelson, we defined a geometrical baseline connecting the anterior and posterior borders of the CC (Fig. 3, bottom). In accordance with DTI fiber tractography, we then distinguished five vertical partitions of the CC. Region I as the most anterior segment covers the first sixth of the CC and contains fibers projecting into the prefrontal region. The rest of the anterior half of the CC, that is region II, contains fibers projecting to premotor and supplementary motor cortical areas. Together, these callosal fibers occupy the largest subdivision of the CC, which extends far more posteriorly as compared to Witelson's scheme. Region III was defined as the posterior half minus the posterior third and comprises fibers projecting into the primary motor cortex. This finding is in clear contrast to Witelson's scheme, which postulates that primary motor fibers cross the CC in the anterior half. Region IV, the posterior one-third minus posterior one-fourth, refers to primary sensory fibers. Callosal parietal, temporal, and occipital fibers cross the CC through region V, which is defined as the posterior one-fourth.

In summary, the new segmentation of the midsagittal CC differs from Witelson's scheme mainly at the anterior tip and the broad midbody area. It may serve as a template for future anatomical and MRI studies, especially when studying callosal fibers connecting to primary motor and sensory cortical areas.

Fractional anisotropy and microstructure of the corpus callosum

As can be appreciated in the grayscale FA maps in Fig. 2 (left columns), there are consistent differences in diffusion anisotropy across the CC in all subjects. The most pronounced anisotropy was found in anterior and posterior regions of the CC with the highest FA values close to 0.8 in the most posterior area and the lowest values between 0.25 and 0.5 in the middle region. Although the absolute anisotropy varied between subjects, its regional distribution along the CC appeared very similar. Hence, Fig. 4 compares normalized FA values averaged across subjects

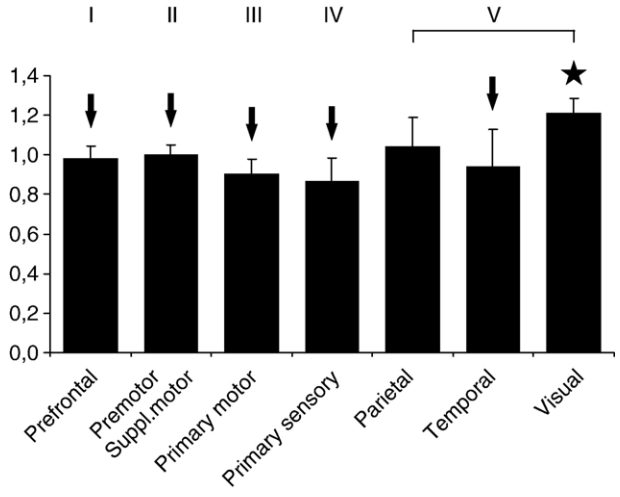

Fig. 4. Normalized mean fractional anisotropy averaged across subjects ($n = 8$) within different regions of the corpus callosum (numbers follow the proposed scheme in the bottom part of Fig. 3). The asterisk indicates significant differences ($P < 0.05$) of the occipital region to other regions (arrows).

for those CC regions that tractography identified to connect specific cortical projection areas. The lowest anisotropy was observed in regions III and IV assigned to primary motor and sensory cortical areas, respectively. The normalized FA values of the callosal occipital (visual) region were significantly different ($P < 0.05$) to those in all other regions except for the parietal segment.

In general, water diffusion anisotropy as determined by MRI reflects a number of microstructural parameters such as the thickness of the individual myelinated axons, the density of respective fibers, and the presence of obliquely oriented fibers in an image voxel. In view of these factors, one may conclude that the available histological data are in general agreement with the measured FA distribution in the human CC. Previous studies already assumed a correlation between the degree of diffusion anisotropy in the CC and the microstructure of fiber bundles (Chepuri et al., 2002; Oh et al., 2005). Using light and electron microscopy techniques, Aboitz and colleagues (1992) reported fibers with a relatively small diameter to be concentrated in the anterior (region I) and posterior part (region V) of the CC. In particular, the latter finding is in qualitative agreement with the highest FA values in the most posterior part of the CC representing occipital (visual) fiber bundles (see Fig. 4). Not only lead thin fibers to a more severe restriction in water mobility, but also a high density of mostly parallel axon bundles reinforces the MRI-detectable effect. Densely packed and lightly myelinated thin fibers (<0.4 μm diameter) are also found in the genu of the CC (region I). The fact that their FA values are slightly lower than in region V may be explained by the presence of a greater number of non-parallel, obliquely oriented fibers that connect heterotopic cortex regions of both hemispheres (Chepuri et al., 2002). Less densely packed fibers with considerably larger diameters (>3 μm) are mainly concentrated in the posterior midbody, that is in regions III and IV of the proposed classification and represent callosal connections to primary motor and sensory areas. Their structural differences are in line with the observation of the lowest FA values.

Concluding remarks

DTI of water molecules within the human brain offers unique access to the microstructure of white matter in vivo (Basser and Pierpaoli, 1996). Here, by means of DTI-based fiber tractography, the topographic arrangement of transcallosal fiber tracts projecting into specific cortical areas was re-evaluated, and striking differences were found to previous classifications in a consistent manner. Nevertheless, current methodologies still face a number of challenges. As an example, lateral projections of the CC were difficult to resolve. A possible explanation is the simultaneous presence of multiple fiber bundles in respective image voxels that possess different orientations such as contributions from the association fibers located lateral to the CC. These problems must be ascribed to the still rather coarse spatial resolution, the inherent assumptions of the diffusion tensor model, and the use of a rather simplistic tract-tracing algorithm. In fact, the achievable voxel resolution and the access to a true 3D distribution of the water diffusivity − both within measuring times suitable for human in vivo studies − present the main limitations of the approach chosen here.

Partial volume effects due to the use of voxel sizes larger than the typical diameter of a specific fiber bundle (or tract) result in apparently reduced diffusion anisotropy and correspondingly lower FA values by averaging white matter tracts with more isotropic tissues such as gray matter or even CSF. Moreover, there are limitations of the simple diffusion tensor model if fibers merge, branch, or cross. In these cases, the assumption of a single major diffusion direction fails and again yields apparently lower mean anisotropy measures that refer to an inadequate isotropic compromise of a complex 3D distribution of water diffusivity with two or more maxima. The immediate consequence for fiber tractography is either a false-positive directional choice for a continuation of the tract-tracing algorithm or a full stop by reaching the lower anisotropy threshold. The FACT algorithm used here can be easily extended by adding more sophisticated boundary conditions or anatomy-derived ‘rules’. For example, the inclusion of curvature information from the already established part of the trajectory into the continuation decision may considerably improve the tracking of fibers that are more bended than transcallosal connections.

Although the aforementioned challenges emerge as a general concern for fiber tractography, they did not arise as a major obstacle for studying the topology of fiber connections in the human CC. In fact, the use of a conservative algorithm helped to reduce putatively false-positive tract contributions. The resulting scheme for a new CC segmentation offers a valid base for clinical applications, in particular for MRI studies of neurodegenerative disorders that affect the transcallosal connectivity. Nevertheless, future more detailed work on white matter fiber anatomy would substantially benefit from access to improved spatial resolution of DTI acquisitions as well as from an even greater number of diffusion-encoding gradients and a more adequate representation of orientational distributions.

Acknowledgments

SH was supported by the Bundesminister für Bildung und Forschung of the Federal Republic of Germany (grant 01 GQ 0432). The authors thank Matthias Küntzel for his software developments and helpful comments regarding the manuscript.

References

Aboitz, F., Scheibel, A.B., Fisher, R.S., Zaidel, E., 1992. Fiber composition of the human corpus callosum. Brain Res. 598, 143–153.

Basser, P.J., Pierpaoli, C., 1996. Microstructural and physiological features of tissues elucidated by quantitative diffusion-tensor MRI. J. Magn. Reson., B 111, 209–219.

Chepuri, N.B., Yen, Y.F., Burdette, J.H., Li, H., Moody, D.M., Maldjian, J.A., 2002. Diffusion anisotropy in the corpus callosum. Am. J. Neuroradiol. 23, 803–808.

Clarke, J.M., Zaidel, E., 1994. Anatomical–behavioral relationships: corpus callosum morphometry and hemispheric specialization. Behav. Brain. Res. 64, 185–202.

De Lacoste, M.C., Kirkpatrick, J.B., Ross, E.D., 1985. Topography of the human corpus callosum. J. Neuropathol. Exp. Neurol. 44, 578–591.

Dougherty, R.F., Ben-Shachar, M., Bammer, R., Brewer, A.A., Wandell, B.A., 2005. Functional organization of human occipital–callosal fiber tracts. Proc. Natl. Acad. Sci. U. S. A. 102, 7350–7355.

Duara, R., Kushch, A., Gross-Glenn, K., Barker, W.W., Jallad, B., Pascal, S., Loewenstein, D.A., Sheldon, J., Rabin, M., Levin, B., 1991. Neuroanatomic differences between dyslexic and normal readers on magnetic resonance imaging scans. Arch. Neurol. 48, 410–416.

Huang, H., Zhang, J., Jiang, H., Wakana, S., Poetscher, L., Miller, M.I., van Zijl, P.C., Hillis, A.E., Wytik, R., Mori, S., 2005. DTI tractography based parcellation of white matter: application to the mid-sagittal morphology of corpus callosum. NeuroImage 15, 195–205.

Lacerda, A.L., Brambilla, P., Sassi, R.B., Nicoletti, M.A., Mallinger, A.G., Frank, E., Kupfer, D.J., Keshavan, M.S., Soares, J.C., 2005. Anatomical MRI study of corpus callosum in unipolar depression. J. Psychiatr. Res. 39, 347–354.

Larsen, J.P., Høien, T., Ödegaard, H., 1992. Magnetic resonance imaging of the corpus callosum in developmental dyslexia. Cogn. Neuropsychol. 9, 123–134.

Mori, S., Crain, B.J., Chacko, V.P., van Zijl, P.C., 1999. Three-dimensional tracking of axonal projections in the brain by magnetic resonance imaging. Ann. Neurol. 45, 265–269.

Narr, K.L., Cannon, T.D., Woods, R.P., Thompson, P.M., Kim, S., Asunction, D., van Erp, T.G., Poutanen, V.P., Huttunen, M., Lonnqvist, J., Standerksjold-Nordenstam, C.G., Kaprio, J., Mazziotta, J.C., Toga, A.W., 2002. Genetic contributions to altered callosal morphology in schizophrenia. J. Neurosci. 22, 3720–3729.

Nolte, U.G., Finsterbusch, J., Frahm, J., 2000. Rapid isotropic diffusion mapping without susceptibility artifacts. Whole brain studies using diffusion-weighted single-shot STEAM MR imaging. Magn. Reson. Med. 44, 731–736.

Oh, J.S., Suk Park, K., Chan Song, I., Ju Kim, S., Hwang, J., Chung, A., Kyoon Lyoo, I., 2005. Fractional anisotropy-based divisions of midsagittal corpus callosum. NeuroReport 16, 317–320.

Oldfield, R.C., 1971. The assessment and analysis of handedness: the Edinburgh Inventory. Neuropsychologia 9, 97–113.

Plessen, K.J., Wentzel-Larsen, T., Hugdahl, K., Feineigle, P., Klein, J., Staib, L.H., Leckman, J.F., Bansal, R., Peterson, B.S., 2004. Altered interhemispheric connectivity in individuals with Tourette's disorder. Am. J. Psychiatry 161, 2028–2037.

Rajapakse, J.C., Giedd, J.N., Rumsey, J.M., Vaituzis, A.C., Hamburger, S.D., Rapoport, J.L., 1996. Regional MRI measurements of the corpus callosum: a methodological and developmental study. Brain Dev. 18, 379–388.

Ramnani, N., Behrens, T.E., Penny, W., Matthews, P.M., 2004. New approaches for exploring anatomical and functional connectivity in the human brain. Biol. Psychiatry 56, 613–619.

Rieseberg, S., Merboldt, K.D., Küntzel, M., Frahm, J., 2005. Diffusion tensor imaging using partial Fourier STEAM MRI with projection onto convex subsets reconstruction. Magn. Reson. Med. 54, 486–490.

Teipel, S.J., Schapiro, M.B., Alexander, G.E., Krasuski, J.S., Horwitz, B., Hoehne, C., Moller, H.J., Rapoport, S.I., Hampel, H., 2003. Relation of corpus callosum and hippocampal size to age in nondemented adults with Down's syndrome. Am. J. Psychiatry 160, 1870–1878.

Thompson, P.M., Narr, K.L., Blanton, R.E., Toga, A.W., 2003. Mapping structural alterations of the corpus callosum during brain development and degeneration. In: Zaidel, E., Iacoboni, M. (Eds.), The Parallel Brain: The Cognitive Neuroscience of the Corpus Callosum, pp. 93–130.

Thompson, P.M., Dutton, R.A., Hayashi, K.M., Lu, A., Lee, S.E., Lee, J.Y., Lopez, O.L., Aizenstein, H.J., Toga, A.W., Becker, J.T., 2006. 3D mapping of ventricular and corpus callosum abnormalities in HIV/AIDS. NeuroImage 13, 12–23.

von Plessen, K., Lundervold, A., Duta, N., Heiervang, E., Klauschen, F., Smievoll, A.I., Ersland, L., Hugdahl, K., 2002. Less developed corpus callosum in dyslexic subjects-a structural MRI study. Neuropsychologia 40, 1035–1044.

Weis, S., Kimbacher, M., Wegner, E., 1993. Morphometric analysis of the corpus callosum using MR: correlation of measurements with aging in healthy individuals. Am. J. Neuroradiol. 14, 637–645.

Witelson, S.F., 1989. Hand and sex differences in the isthmus and genu of the human corpus callosum. A postmortem morphological study. Brain 112, 799–835.